Magnetic Properties of the Gd-La and Gd-Y Alloys*

W. C. THOBURN, S. LEGVOLD, AND F. H. SPEDDING
Institute for Atomic Research and Department of Physics, Iowa State College, Ames, Iowa
(Received February 18, 1958)

Magnetic properties of Gd-La and Gd-Y alloys are presented. For alloys of high Gd content, paramagnetic to ferromagnetic transitions are observed with decreasing temperature. As the Gd content is decreased, ferromagnetic ordering is replaced by antiferromagnetic ordering. In the Gd-La alloys, a crystal structure change affects the magnetic properties.

I. INTRODUCTION

THE magnetic properties of gadolinium metal have been reported by a number of investigators.[1–4] Since the 4*f* shell, which contains the electrons of unpaired spin in the rare earths, is so well shielded by outer electrons, direct interaction between the 4*f* electrons of neighboring atoms must be small. Thus it seems that interactions through the conduction electrons must help to determine the magnetic properties of the metal. Nearest-neighbor and next-nearest-neighbor interactions are consequently of interest. One approach to an understanding of the long-range interactions is through a study of alloys.

We present here findings on the magnetic properties of alloys of gadolinium and each of two weakly paramagnetic metals—lanthanum, the beginning element of the rare-earth series with no 4*f* electrons, and yttrium, the trivalent fourth-period element which has the same crystal structure as gadolinium and nearly the same atomic volume.

II. MATERIALS STUDIED

The alloys examined in this study were prepared in the Ames Laboratory of the U. S. Atomic Energy Commission by fusing together carefully weighed amounts of the constituents in a tantalum crucible. The heating was done in an atmosphere of pure argon in an induction furnace. The pure elements were prepared by methods previously reported.[5,6]

The alloys were tested spectrographically and chemically for impurities (see Table I) and also examined with x-rays to ascertain their crystal structures.

The results of the x-ray examination of the alloys are shown in Table II. Lattice parameters for the pure metals[7] are shown for comparison.

TABLE I. Purity of samples.

Percent of Gd	Amounts of impurities (parts per million): Spectrographic estimates[a]	Chemical analysis
Diluent lanthanum:		
46.6	nil	nil
75	Ta, 200	C, 371 N, 198
83.3	Y, 2000; Cu, 5000; Fe, Si, Cr, 100	C, 198 N, 256
90	Cu, Al, Ca, Fe, Mg, Mn, Si, Y, Yb, 100	C, 174 N, 258
Diluent yttrium:		
25	Ta, 500; Al, Cu, Fe, Si, Sm, Cr, 100	C, nil N, 353
50	Yb, 100	C, 313 N, 230
60	Fe, 200; Al, Be, Mg, Mn, Ni, Si, 100	C, 131 N, 201
66.7	Fe, 500; Al, Cu, Si, Sn, Cr, 100	C, 61 N, 450
75	Ta, 200; Ca, Fe, Cu, 100	C, 174 N, 237
83.3	Ta, 200; Ca, 100	C, 192 N, 261
90	Ta, 200; Ca, 100	C, 334 N, 205

[a] The figures represent upper limits. Complete spectrographic standards for evaluating the impurities for these alloys were not available.

III. METHOD OF MEASUREMENT

The experimental procedure and equipment used in this work has been described by Elliott, Legvold, and Spedding.[3] The magnet was improved by the addition of a current control which held the field constant within one oersted, and the pole pieces were reground to give a more uniform field gradient. For measurements in the ferromagnetic temperature range, samples 1 mm×1 mm ×10 mm were employed. In the paramagnetic and antiferromagnetic ranges, larger cylindrical samples, 5 mm in diameter and 1 cm long, were used.

For most of the measurements the sample was placed in the gas stream above a vessel of boiling liquid nitrogen or liquid hydrogen. A heater in the gas stream was used to obtain temperatures up to 350°K. In addition, measurements were made in baths of liquid hydrogen and liquid helium.

TABLE II. Alloy crystal structures.

Alloy	Structure	Stacking	Lattice parameters in A: *a*	*c*
Gd-La alloys:				
46.6% Gd	h.c.p. (double axis)	*abacab*···	3.71	11.96
75 and 83.3% Gd	h.c.p. (multiple axis)	unknown	3.66	*n*(5.86)
90% Gd	h.c.p.	*ababa*···	3.65	5.81
Gd-Y alloys (all)	h.c.p.	*ababa*···	3.64	5.76
Pure yttrium	h.c.p.	*ababa*···	3.6474	5.7306
Pure lanthanum	h.c.p. (double axis)	*abacab*···	3.770	12.159
Pure gadolinium	h.c.p.	*ababa*···	3.636	5.7826

* Contribution No. 577. Work was performed in the Ames Laboratory of the U. S. Atomic Energy Commission.

[1] G. Urbain *et al.*, Compt. rend. **200**, 2132 (1935).
[2] F. Trombe, Ann. phys. **7**, 383 (1937).
[3] Elliott, Legvold, and Spedding, Phys. Rev. **91**, 28 (1953).
[4] Legvold, Spedding, Barson, and Elliott, Revs. Modern Phys. **25**, 129 (1953).
[5] F. H. Spedding *et al.*, J. Am. Chem. Soc. **69**, 2777 and 2812 (1947).
[6] A. H. Daane and F. H. Spedding, J. Electrochem. Soc. **100**, 442 (1953).
[7] F. H. Spedding *et al.*, Acta Cryst. **9**, 559 (1956).

IV. RESULTS

Four alloys of gadolinium with lanthanum and seven with yttrium were examined. Alloy proportions are expressed throughout in terms of the atomic percentage of gadolinium. Results for the alloys with lanthanum are presented first.

An alloy of 47% Gd (and 53% La) showed simple paramagnetism down to 20.4°K, and followed the Curie law. A lowered value of σ for low fields in the helium bath indicated the possibility of a transition to antiferromagnetism at some temperature below 20°K.

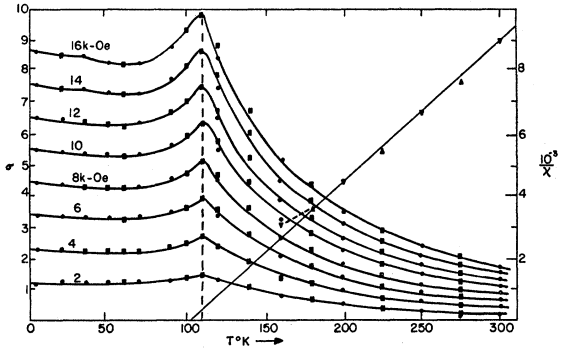

FIG. 1. Magnetic moment per gram (emu) *vs* T, and $1/x$ *vs* T, for the 25% Gd–75% Y alloy. (Squares and dots indicate observations made on different runs.)

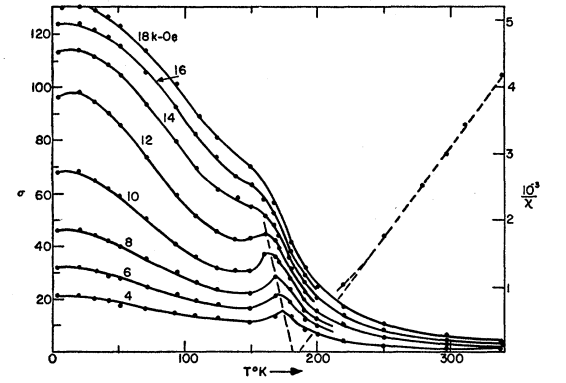

FIG. 2. Magnetic moment per gram (emu) *vs* T, and $1/x$ *vs* T, for the 50% Gd–50% Y alloy. The Néel point for zero field is obtained by projecting the dashed line of the peaks to the temperature axis.

A 90% alloy was ferromagnetic below 258°K, and extrapolations to infinite field and 0°K indicated a saturation moment $\sigma_{\infty,0}=234$ cgs units. The two intermediate compositions showed poorly defined antiferromagnetic maxima at about 130°K and 155°K, apparently corresponding to a composition-dependent transition from the lanthanum to the gadolinium structure as indicated in Table II.

The close similarity of Gd and Y in structure and atomic dimensions indicated that yttrium should be a better diluent for gadolinium. The alloys with yttrium

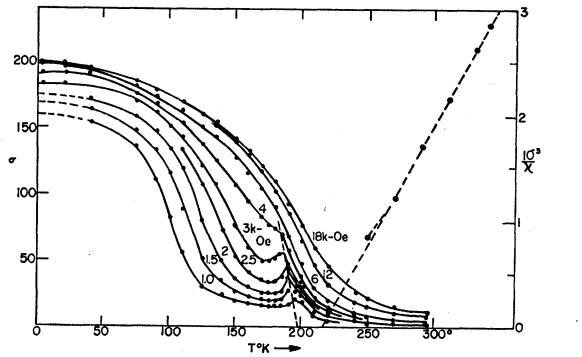

FIG. 3. Magnetic moment per gram (emu) *vs* T, and $1/x$ *vs* T, for the 60% Gd–40% Y alloy. As is usual near the lower limit of paramagnetic disorder, the plot of $1/x$ *vs* T departs from the straight line whose extension gives the paramagnetic Curie point.

ranged in gadolinium content by atoms from 25 to 90%. Typical curves showing the specific magnetization σ as a function of the temperature for various effective fields are shown in Figs. 1, 2, 3, and 4. It is seen that the first three figures show antiferromagnetism at low temperatures, but that as the gadolinium content increases, the antiferromagnetic ordering is progressively more easily overcome by the magnetic field. With 60% gadolinium, the change from antiferromagnetism to ferromagnetism is induced by a field of 4 kilo-oersteds, and below 95°K ferromagnetism appears. We note that while the Néel point or temperature of the antiferromagnetic peak is practically unaffected by the field in the 25% alloy, the Néel points for the alloys of greater Gd content are clearly shifted to lower temperatures by increasing fields.

The remaining alloys with yttrium, having 67 to 90% of Gd by atoms, all showed transitions from ferromagnetism to paramagnetism at well-defined ferromagnetic Curie points as given in Table IV. None showed antiferromagnetism. The curves of Fig. 4 are typical of these alloys and of the 90% Gd-La alloy. The curves for the others are similar in character, and indicate a regular increase in saturation moments and Curie points with increasing gadolinium content.

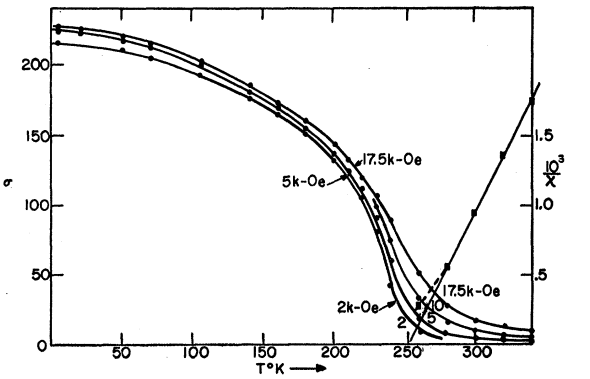

FIG. 4. Magnetic moment per gram (emu) *vs* T, and $1/x$ *vs* T, for the 75% Gd–25% Y alloy.

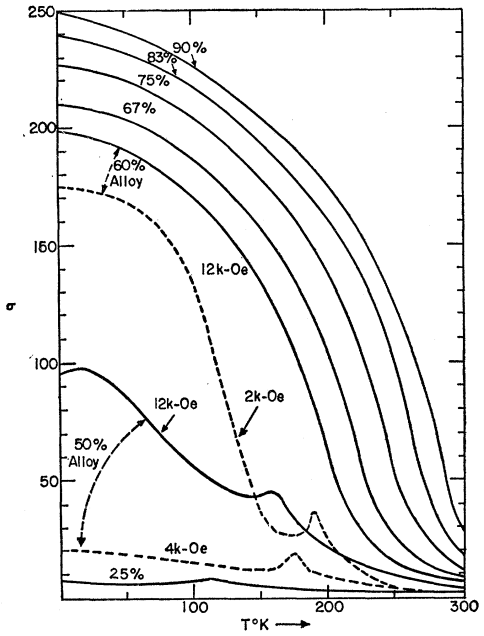

FIG. 5. Comparison of Gd-Y alloys. Alloys are identified by the percent of Gd by atoms. All the solid curves are for a field of 12 kilo-oersteds.

In Fig. 5 are shown σ *vs* T curves for all the Gd-Y alloys under a field of 12 kilo-oersteds on the same scale.

TABLE III. Antiferromagnetic and paramagnetic results.

Alloy	Percent of Gd (atoms)	Néel point (°K)	θ_p (°K)	$C\times10^3$ (deg/cgs)	μ_A (β units)
Gd-La:					
	46.6	18(?)±5	−3±2	30.0	8.70±0.06
	75	130±5	70±5	43.2	8.38±0.15
	83.3	155±5	172±8	34.5	7.14±0.4
	90		260±2	53.3	8.70±0.2
Gd-Y:					
	25	111±2	102±2	22.1	8.66±0.1
	50	182±2	186±3	36.7	8.49±0.2
	60	197±2	217±1	43.0	8.63±0.1
	66.7		229±2	48.6	8.84±0.2
	75		252±1	50.0	8.65±0.1
	83.3		266±1	54.4	8.72±0.1
	90		280±1	58.6	8.84±0.15
Pure Gd[a]			302.7		7.93

[a] Data taken from reference 2.

TABLE IV. Ferromagnetic results.

Percent of Gd	θ_f (°K)	Sat. moment $\sigma_{\infty,0}$ in emu per g of sample	per g of Gd in sample	M_A (β units)
Gd-La:				
90	258±1	234 ±1	257	7.22±0.03
Gd-Y:				
60	95±2	201.3±1	277.4	7.79±0.03
66.7	211±1	211.6±1	271.6	7.63±0.03
75	241±1	228.6±1	271.8	7.63±0.03
83.3	262±1	241.3±1	268.7	7.55±0.03
90	281±1	250.2±1	266.0	7.47±0.03
Pure Gd[a]	289±1	253.6±0.6	253.6	7.12±0.02

[a] Data taken from reference 3.

Also shown are dotted curves which bring out the antiferromagnetic behavior of the 50 and 60% alloys at lower fields.

The significant characteristic temperatures and magnetic moments for the various alloys are listed in Tables III and IV. The last column of each table gives the magnetic moment per Gd atom in Bohr magnetons. In Table III the number of Bohr magnetons, μ_A, is computed from the Curie constant C obtained from the slope of the $1/\chi$ *vs* T straight-line plot at the right of each of the graphs represented by Figs. 1 to 4. Here χ

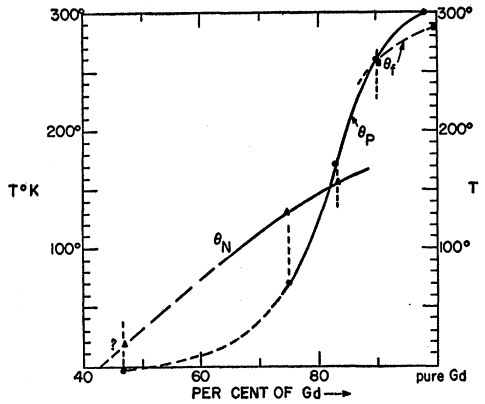

FIG. 6. Significant temperatures of Gd-La alloys. θ_p, θ_f, and θ_N are the paramagnetic and ferromagnetic Curie points and the Néel point, respectively. Vertical dashed lines indicate compositions studied. Dashed portions of curves are estimated.

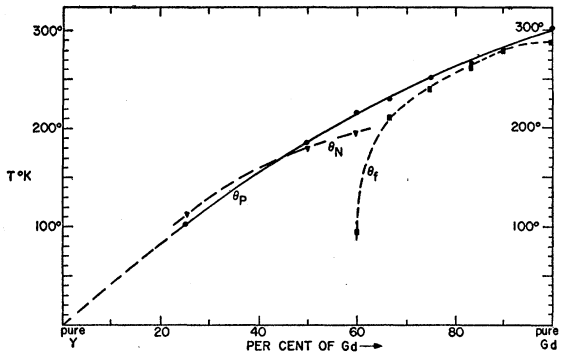

FIG. 7. Significant temperatures of Gd-Y alloys. θ_p, θ_f, and θ_N are the paramagnetic, ferromagnetic Curie points, and the Néel point, respectively. The dashed portion of the θ_p curve is an extrapolation.

is the mass susceptibility. In Table IV, M_A is calculated from the saturation moment $\sigma_{\infty,0}$, and represents the ferromagnetic moment per atom.

Figures 6 and 7 show the paramagnetic and ferromagnetic Curie points, θ_p and θ_f, and the Néel points θ_N plotted against atomic percentage of Gd atoms.

V. DISCUSSION

It is seen that the experimentally determined values of both μ_A and M_A are significantly higher than the

theoretical values for gadolinium obtained on the assumption of contributions by spin only. These are, respectively, $\mu_A = g[J(J+1)]^{\frac{1}{2}} = 7.94$ and $M_A = gJ = 7.00$ in Bohr magnetons, where for gadolinium the Lande factor g is 2 and the total angular momentum quantum number J has the value $\frac{7}{2}$. It appears that the presence of the diluent either brings into play contributions to magnetism by orbital moments, or alters the probability of transfers from the conduction-band electrons in a manner favoring an increased magnetic moment.

It is noteworthy that, except for the marked departures in the neighborhood of 60% Gd concentration, the Néel points θ_N and ferromagnetic Curie points θ_f of the alloys with yttrium tend to be close to the corresponding paramagnetic Curie points θ_p. Dilution with yttrium appears to change the magnetic properties of gadolinium for the most part continuously.

The authors wish to acknowledge the assistance of Mr. Robert Johnson who prepared the alloys and examined their structures.

PHYSICAL REVIEW VOLUME 110, NUMBER 6 JUNE 15, 1958

Lifetime in p-Type Silicon

J. S. BLAKEMORE
Honeywell Research Center, Hopkins, Minnesota
(Received June 10, 1957; revised manuscript received January 24, 1958)

By using the photoconductive decay method, lifetime is measured as a function of excess electron density in p-type silicon over the temperature range 200–400°K. The linear dependence of τ_n on Δn expected from the Shockley-Read theory of recombination is not obeyed; instead a much stronger dependence is found with minority carrier densities less than 10^{12} cm^{-3} than at larger densities. The data are discussed in terms of two separate recombinative levels of the Shockley-Read type of of more complex behavior for a single kind of center.

I. INTRODUCTION

OF the parameters which characterize the bulk behavior of a semiconductor, minority carrier lifetime is one of the most important, and many methods have been devised for its measurement. Unfortunately, various measurements on a single sample do not always agree, since there are two ways in which ambiguity can arise.

Firstly, the extent to which surface recombination adds to that of the bulk depends on the details of the experimental arrangement, and due attention must be paid to minimizing this perturbation. Secondly, we must note that in some materials, of which p-type silicon is a good example, bulk lifetime varies with the density of excess minority carriers and is meaningful only when expressed together with the corresponding carrier concentration.

Thus in p-type silicon it is desirable to measure the lifetime τ_n as a function of electron density Δn. Such measurements have been reported for one specimen by Bemski[1] who found a linear dependence of τ_n on Δn as expected from the Shockley-Read theory of recombination centers.[2] In brief reports on the work described in this paper,[3] it was noted that the dependence can depart from linearity, suggesting the influence of more than one recombinative level.

[1] G. Bemski, Phys. Rev. **100**, 523 (1955).
[2] W. Shockley and W. T. Read, Phys. Rev. **87**, 835 (1952).
[3] J. S. Blakemore, Bull. Am. Phys. Soc. Ser. II, **2**, 153 (1957); **3**, 101 (1958).

II. EXPERIMENTAL ARRANGEMENT

Lifetime was measured from the time constant of photoconductive decay following 0.7-μsec pulses of light from a spark gap. Specimens were operated under constant-current conditions so that a transient voltage was developed on illumination. This was amplified and displayed on a Tektronix 514AD oscilloscope. In operation, the preamplifier gain and oscilloscope sweep rate were varied to match the photoconductive decay against an exponential curve drawn on the cathode ray tube face (Fig. 1). Since the decay is not a pure exponential, the time base speed was found for which a coincidence occurred between the drawn exponential and one section of the decay. From the sweep speed (which can be read directly on this

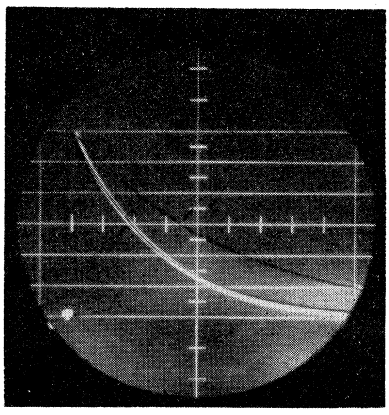

FIG. 1. Oscilloscope trace of photoconductive decay in p-type silicon. The time base is adjusted for coincidence between a portion of the trace and one of the two black exponential marker curves.